Journal of Agricultural and Marine Sciences 2021, 26(1): 37–46
DOI: 10.24200/jams.vol26iss1pp37-46
Reveived 17 Feb 2020
Accepted 22 Aug 2020

RESEARCH PAPER

Mean Sea Level Variability along the Northern Coast of the Oman Sea and its Response to Monsoon and the North Atlantic Oscillation Index from Tide Gauge Measurement

S. Hassanzadeh[1,*], F. Hosseinibalam[1]

متوسط التباين في مستوى سطح البحر على طول الساحل الشمالي لبحر عمان واستجابته للرياح الموسمية ومؤشر تذبذب شمال الأطلسي من مقياس المد والجزر

س. اسمعيل حسن زاده و ف. حسينى بالام

Abstract. Sea level analysis along the Northern Coast of the Oman Sea was investigated on the basis of tide gauge measurements. Meteorological parameters, along with monsoon and NAO (North Atlantic Oscillation) indices were used to study the response of sea level to local and global forcing. The relation between sea level and forces were examined. Low correlation coefficient (-0.35) between sea level and atmospheric pressure at Chabahar indicated that the response to atmospheric pressure was not an inverse barometric. The nature of local inverse barometric effects were examined through a series of statistical models. Analysis between sea level and atmospheric pressure reveals a significant coherence, which meant that along the Northern Coast of Oman Sea, mean sea level responded to atmospheric pressure as an inverse barometer. It can be noticed that the difference between atmospheric pressure and mean sea level was due to alongshore wind stress forcing and was consistent with that expected from Ekman dynamics. The four EOF modes capture 87.16% for the x-component and 94.70% for the y-component of the total variance and were statistically significant. Linear regression and ARIMA model forecasts were fitted to sea level and compared to the actual data. Even though both models gave similar results, the ARIMA model performed considerably better.

Keywords: The Oman Sea, Tide Gauge, ARIMA, Monsoon

المستخلص: تم تحليل مستوى سطح البحر على طول الساحل الشمالي لبحر عمان على أساس قياسات المد والجزر، حيث استخدمت مؤشرات الأرصاد الجوية إلى جانب مؤشرات الرياح الموسمية وتذبذب شمال الأطلسي لدراسة استجابة مستوى سطح البحر للتأثيرات المحلية والعالمية وفحص العلاقة بينها وبين مستوى سطح البحر. ووجد أن معامل الارتباط المنخفض (-٠,٣٥) بين مستوى سطح البحر والضغط الجوي في تشابهار يشير إلى أن الاستجابة للضغط الجوي لم تكن تأثيرات جوية معكوسة، حيث تم فحص طبيعة التأثيرات الجوية العكسية المحلية من خلال سلسلة من النماذج الإحصائية، وقد كشف التحليل بين مستوى سطح البحر والضغط الجوي عن وجود تماسك كبير، مما يعني أن متوسط مستوى سطح البحر على طول الساحل الشمالي لبحر عمان قد استجاب للضغط الجوي بشكل عكسي، وقد لوحظ أن الفرق بين الضغط الجوي ومتوسط مستوى سطح البحر حدث بسبب تأثير إجهاد الرياح على طول الشاطئ والذي كان متسقًا مع المتوقع من ديناميكيات إيكمان، ووجد أن أوضاع EOF الأربعة قد إلتقطت ما مقداره ٨٧,١٦٪ للمكون x و ٩٤,٧٠٪ للمكون y من التباين الإجمالي والتي كانت ذات دلالة إحصائية، وقد تم ضبط الانحدار الخطي وتوقعات نموذج ARIMA على مستوى سطح البحر ومقارنتها بالبيانات الفعلية، وعلى الرغم من أن كلا النموذجين أعطيا نتائج مماثلة إلا أن أداء نموذج ARIMA كان الأفضل.

الكلمات المفتاحية: الكلمات المفتاحية: بحر عمان، مقياس المد والجزر، ARIMA ، الرياح الموسمية

Introduction

The coastal environment is very vulnerable to the changes in the mean sea level, wave heights and wave direction. Many forces in the atmosphere and the ocean influence the sea level. Thus, the sea level integrates a great number of physical processes in the environment and therefore can be a representative parameters for monitoring the relationship between oceanic and atmospheric parameters. This study of sea-level variability is usually undertaken from hindcasts of the last decades (Somot et al., 2006) and from the available tide gauges and satellite altimeters data. Sea level changes can be divided into dynamic and quasi-static components (Stammer et al., 2013). For various reasons, the sea level can be changed quite differently from one region to another (Ding et al., 2001). According to Eshghi et al. (2020), the inverted barometer effect was significant in the north-western Indian Ocean. Siddig et al. (2019) estimated the linear trend using monthly mean residual sea level and they found the highest trend values was at Mina Salman about 3.4 0±0.98 mm/year and Abu Ali Pier about 3.1±0.7 mm/year. Therefore, it is necessary to study the sea level changes locally or regionally to understand the various geophysical processes associated with the sea level variability. The Oman Sea, also called the Oman Gulf, is located at the north of the Arabian Sea (Figure 1).

The Gulf of Oman is strongly influenced by outflow from the Hormuz Strait. From fall through mid-spring,

Smaeyl Hassanzadeh[1,*](✉) shz@phys.ui.ac.ir, Department of physics, University of Isfahan, 81746-73441, Isfahan, Iran,[1] Department of physics, University of Isfahan, 81746-73441, Isfahan, Iran

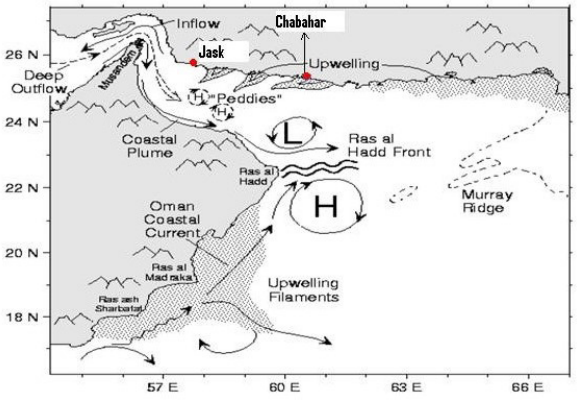

Figure 1. Circulation of the Oman Sea and Northern Arabian Sea and the location of the Tide Gauge, Chabahar and Jask (Johns et al., 1999)

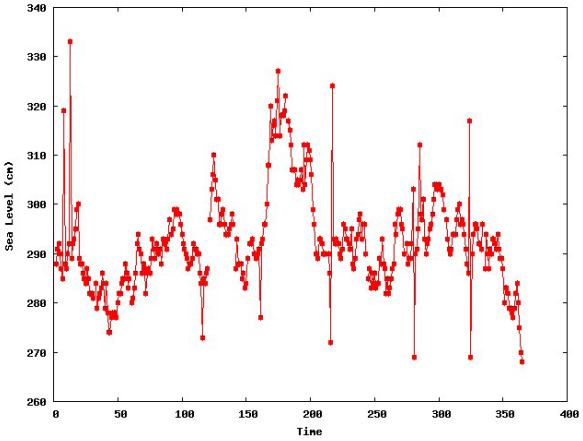

Figure 2. Hourly sea level variability at Chabahar on the north coast of the Oman Sea

satellite SSTs suggested a plume of outflow water owing as a coastal current along the Oman and Emirate coast to Ras al Hadd at the edge of the Arabian Sea (Johns et al., 1999). This would imply that at least through part of the year this outflow from the Hormuz Strait consists of deep water layer and a modified surface layer that must together balance the inflow component. The seasonal upwelling and circulation are also important along the coast of Iran in the Oman Sea. The seasonal and inter-annual variations in the circulation of the Gulf of Oman is significant (Figure 1). The northern side of the Gulf of Oman has consistent upwelling associated with the SW monsoon along the Pakistani coast (Figure 1). Upwelling along the western, Iranian coast is more variable.

In 1995, for example, this coast was associated with upwelling filaments that moved to the west and even entered the outer edges of the Strait of Hormuz. Other years suggest less extensive upwelling although there is localized upwelling at the mouth of the Strait in all the years examined. In this study, data from two tide gauges and meteorological parameters in the Oman Sea as well as data set of the gridded Ekman transport, the North Atlantic Oscillation (NAO) index and the Monsoon index of the Indian Ocean were used.

Methodology

Tide Gauge Data and Mean Sea Level

Hourly time series of tides were obtained from the National Cartographic Center of Iran (NCC) and monthly means of atmospheric parameters were gathered from the Islamic Republic of Iran Meteorological Organization. Atmospheric pressure, air temperature and wind data records were obtained from offshore stations at Chabahar and Jask (Figure 1).

Water level is measured using a mechanical float gauge manufactured by the Ott Companyin Germany. Tidal records were monitored with 30 min sampling and 1 cm resolution. The 30 minute values were converted to hourly values using software developed by NCC. The tide gauges in the Iranian Tide Gauge network were connected to benchmarks established by NCC. NCC did the precise leveling, i.e., they were responsible for determining the vertical distance between the bench marks and the contact point at the tide gauge. The leveling was performed several times every year. The NCC benchmarks were connected to the Iranian National Leveling Network. The tide gauge was calibrated by making its readings equal to the observations on a tide pole installed beside the tidal station. All observations are compared with tidal predictions. If the inspection of the data revealed errors in observed heights, the data were corrected by NCC. NCC used a "modified" Indian Spring Low Water (ISLW) as chart datum. The quality of the Iranian Tide Gauge network was approved by IOC/GLOSS, Technical Report (Hareide, 2004).

The monsoon and NAO indices were obtained from web. Hourly tide gauge data from both Chabahar and Jask stations were used in this study. An example of 1997 tide gauge record at Chahbahar is shown in Figure 2. The daily mean sea levels were calculated by averaging the hourly data of the whole day and are shown in Figure 3. The monthly sea level data available for Chabahar from 1993 to 2005 and for Jask from 1997 to 2005 are shown in Figure 4. Sea level was high in summer and was low in winter at both stations. Interannual variability was also apparent as this appeared relatively coherent between stations.

The annual mean of the sea level at both stations are shown in Figure 5. The highest mean sea level occurred in 1999 and 2004 at Chabahar and in 2003 at Jask. The

annual cycle was common to both tide gauges in the northern coast of the Oman Sea. The seasonal variability had a close relation with the wind and atmospheric pressure. As the monthly data were not removed from this effect, a marked seasonally in monthly average was appeared. The behavior of the seasonal variability is presented in the Figure 6.The seasonal variability in both stations showed a gradual increase in the sea level between February and June, the highest value in June and lowest in January (Figure 6). Then it began to decrease until December at Chabahar and until February at Jask. The ranges were about 14 cm in Chahbar and about 20 cm in Jask. The major peak in June occurred during the southwest monsoon.

Monthly data on sea level, atmospheric pressure, air temperature, sea surface height (SSH), local wind, Monsoon and NAO Indices were analyzed. The monthly and yearly averages for each data set were computed and different statistical analyses were applied. In the first exploratory approach, correlations between sea level and each of the explanatory variables were produced by calculating the Pearson correlation coefficient, and corresponding P-values, between the time series. The empirical orthogonal function (EOF) technique was used to define the patterns of spatial and temporal behavior of the Ekman transport. This technique was also referred to the principal component analysis (PCA). The EOF decomposition was used to extract the dominant modes of spatial and temporal variability of the signal (Preisendorfer, 1988).

Modelling Response and Sea Level Prediction

The role of different climate forcings that might affect the northern coast of the Oman Sea is statistically explored in this section. A linear regression and an Auto-Regressive Integrated Moving Average (ARIMA) model were fit to mean sea level and forcings as predictors for each station and then were used to forecast sea level. The Ekamn transport was first decomposed in its PCs. The ARIMA models are AR models with differencing or moving average terms. The multiple regression was used to observe sea level, SL, as the dependent variable in the regression model of the following form:

$$SL = a\,P + b\,T + c\,W \sum_{i=1}^{N} d_i\,PC_i \qquad \text{Eq.(1)}$$

where independent variables P, T and W are the atmospheric pressure, temperature and wind, respectively, and a, b, and c are the coefficients. PC_i is the ith PC of the Ekman transport and d_i is the corresponding coefficient, and N is the number of PCs included in the model. Owing to possible significant correlation between different sea level forcing inputs, the results from the univariate model are likely to be affected. The statistical way to take the correlation between input forcing into account was to perform a multivariate regression analysis of mean

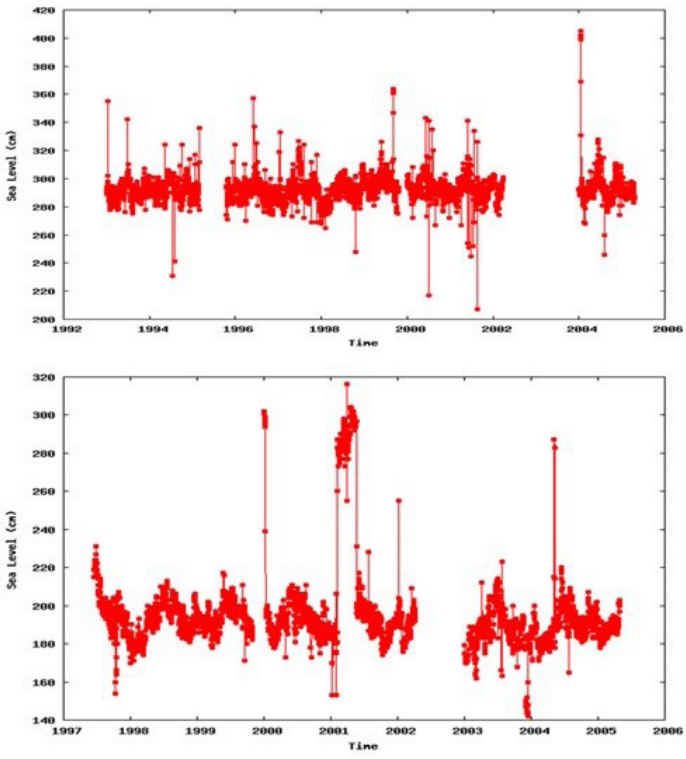

Figure 3. Daily sea level variability at Chabahar (top) and Jask (Bottom) on the north coast of the Oman Sea

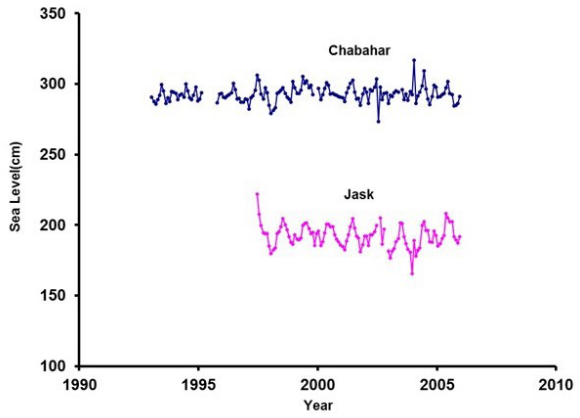

Figure 4. Monthly sea level variability at Chabahar (top) and Jask (Bottom) on the north coast of the Oman Sea

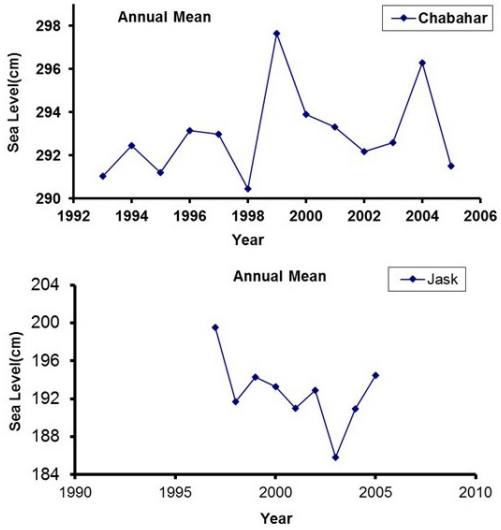

Figure 5. Annual mean sea level at Chabahar (top) and Jask (Bottom)on the north coast of Oman Sea

sea level on predictors.

Multivariate regression was performed to confirm the relationship between sea level and forcing inputs. Thus, regression model enabled to predict sea level using pressure, temperature, wind and Ekman transport forcing. Autoregressive integrated moving average model of degree *p*, *d* and *q*, ARIMA (*p*, *d*, *q*), was a combination of AR and MA with differencing. Where, *p* is the number of autoregressive terms, *d* is the number of non-seasonal differences, and *q* is the number of lagged forecast errors in the prediction equation (Box and Jenkins, 1976). Lags of the differenced series appearing in the forecasting equation are called "auto-regressive" terms, lags of the forecast errors are called "moving average" terms, and a time series which needs to be differenced to be made stationary is said to be an "integrated" version of a stationary series. For non-stationary data one should apply ARMA description to the series of differences of appropriate order, thus yielding ARIMA model (Autoregressive Integrated Moving Average). It can be written as:

$$\varphi(B)\nabla_d X_t = \theta(B)e_t \qquad \text{Eq.(2)}$$

where, ∇_d is a differential operator of degree d: $\nabla_d X_t=(X_t-X_{t-1})_d$. Usually $d = 0,1,2$. A forecast generated by the above process is given by:

$$X_{t+m} = \varphi_1\nabla_d X_{t+m-1} + \cdots + \varphi_{p+d}\nabla_d X_{t+m-p-q} + e_{t+m} - \theta_1 e_{t+m-1} - \cdots - \theta_q e_{t+m-q}$$

Eq.(3)

A forecast with least mean squared error, m periods ahead, is a conditional expected value of random variable X_t in time *t*, which can be written as:

$$\hat{X}_t(m) = E_t[X_{t+m}] = E[X_{t+m}|_{X_t}, X_{t-1}, \ldots] \qquad \text{Eq.(4)}$$

Thus, the forecast is: Eq.(5).

To calculate conditional expected values in the equation above one can assume that:

$E_t[X_{t-j}]=X_{t-j}$, where X_{t-j}, in time t already known, one leaves without changes,

$E_t[X_{t+j}] = \hat{X}_t(j)$,where X_{t+j}, still unknown are replaced with their forecasts $\hat{X}_t(j)$.

$E_t[e_{t-j}]=e_{t-j}$, where e_(t-j), in time *t* already known, one specifies as $X_{t-j} - \hat{X}_{t-j-1}(1)$. Eq.(6)

The monthly data were used to compare the predictive ability of the multiple linear regression based on the predictor variables and ARIMA model based on mean sea level time series. The results of the linear regression model fitting for monthly mean sea level at Chabahar and Jask can be found in Figure 10. The results of the ARIMA model for monthly mean sea level series at Chabahar and Jask are also shown in Figure 10. The ARIMA model was based on time series of the mean sea level using the formula given above. Four ARIMA models with different orders were used to analyze the cases with two Stations for Chabahar from 1993 to 2005 and for Jask from 1997 to 2005. The model parameters including the ARIMA coefficients denoted by p, d, and q are estimated according to the Box-Jenkins methods (Box and Jenkins, 1976) and for Chabahar is shown in Table 1.

The optimal order of the ARIMA models was cho-

$$\hat{X}_t(m) = E_t[X_{t+m}]$$
$$= \varphi_1 \nabla_d E_t[X_{t+m-1}] + \cdots + \varphi_{p+d} \nabla_d E_t[X_{t+m-p-q}] + E_t[e_{t+m}] - \theta_1 E_t[e_{t+m-1}]$$
$$- \cdots - \theta_q E_t[e_{t+m-q}]$$

Eq.(5)

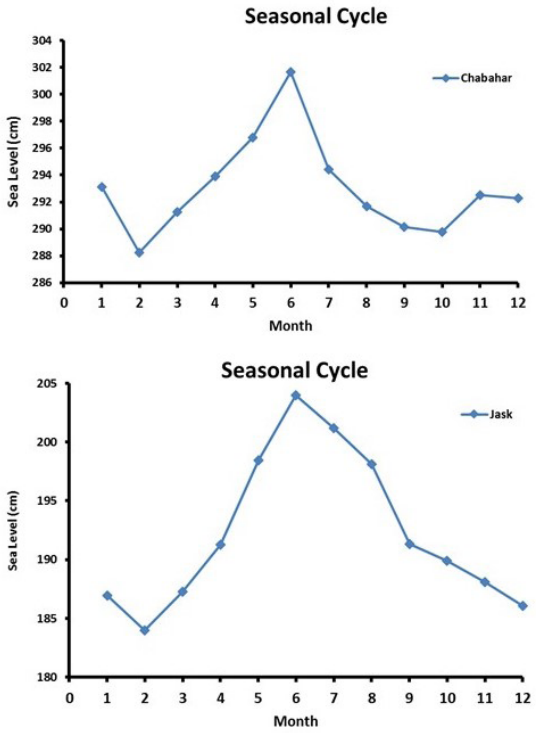

Figure 6. Seasonal change of sea level at Chabahar (top) and Jask (Bottom) on the north coast of Oman Sea

sen by Bayesian Information Criterion (BIC) (Sawa, 1978). Minimum BIC values are used to determine the best performance of the ARIMA model because the BIC places more emphasis on the parsimony of the model. Hence, ARIMA (1, 1, 1) and ARIMA (2, 1, 1), shown in Table 1, were selected to forecast the mean sea level. The predicted of ARIMA (1, 1, 1) models are shown in Fig. 10. The predictions are in agreement with the relevant observations. We compared the forecasting performance of alternative models of the Mean Sea level. Four models are included in the comparison: the ARIMA, models shown in Table 1. Forecasting performance was compared in terms of three criteria: R-Squared, root mean square error (RMSE) and mean absolute percentage error (MAPE). Table 1 summarizes the main diagnostic and forecasting performance measures for the models. The model with the best overall performance is the ARIMA (1.1.1).

In summary, the ARIMA (1,1,1) model has a number of desirable features. All its coefficients are statistically significant, most of them at the 1% level. It can be used to determine the mean sea level. Finally, it has the best forecasting performance of the models considered. Figure 10 shows the similarity between fits of the linear regression and ARIMA models for Chabahar and Jask respectively. Both models predicted seasonality of the data for the sea level. The ARIMA models are more accurate for forecasting the mean sea level than the linear regression models. The two models predicted similar forecasts for sea level, but the greater accuracy for the ARIMA models are attributed to their dynamic nature and their ability to incorporate new information in forecasting by containing lagged terms of the forcing functions as explanatory variables.

Results and Discussion

Effect of Meteorological Parameters on Sea Level Changes

Sea level changes are mainly due to variations in the regional and global meteorological parameters. Atmospheric pressure variations and the thermal effect are the most important caused of sea level changes (Gomis, et al., 2008 and Juncheng, et al., 2009 and Hosseinibalam, et al., 2007). The inverted barometer (IB) effect approx-

Table 1. Testing result of selected Autoregressive Moving Average (ARIMA) models for Chabahar

Structure	BIC (Normalized)	R-Squared	RMSE	MAPE
ARIMA (1, 1, 1)	0.566	0.887	0.684	0.178
ARIMA (2, 1, 1)	0.642	0.889	0.647	0.166
ARIMA (2, 1, 2)	1.199	0.942	0.490	0.109
ARIMA (1, 1, 2)	1.499	0.959	0.415	0.099

Note: BIC (Bayesian Information Criterion), RMSE (Root Mean Square Error, Mean Absolute Percentage Error (MAPE)

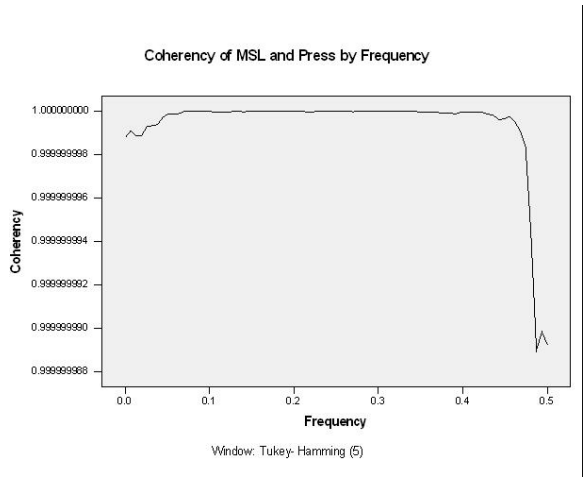

Figure 7. Coherence between mean sea level and atmospheric pressure of the Oman Sea for Chabahar station. Frequency is (cycles/month).

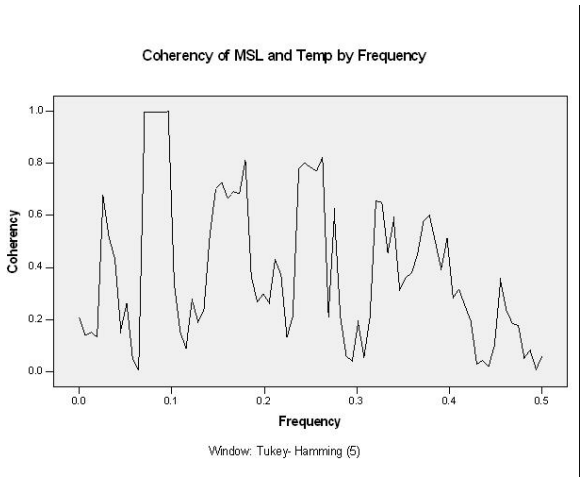

Figure 8. Coherence between mean sea level and air temperature of the Oman Sea for Chabahar station. Frequency is (cycles/month)

imately related the oceanic response to the atmospheric pressure fluctuations. In coastal areas the onshore-offshore wind component can directly push water toward the shore or away from it. Usually the more dominant effect was caused further offshore by the longshore wind component, which can raise or lower the water level because the Coriolis force caused transport to the right of the wind direction. Air temperature affected sea level by warmth caused by the greenhouse effect. A sea level rise could probably be caused by thermal expansion of the water column due to a decrease in water density caused by it being warmed. In a first exploratory approach, correlation coefficients between sea level and each of the above parameters as explanatory variables were found by calculating the Pearson correlation coefficient, and corresponding P-values, between each time series.

Atmospheric Pressure

The correlation coefficient (r) between monthly atmospheric pressure and monthly sea-level data for Chabahar was (r =-0.35) with p-value 0.00 and for Jask is (r =-0.75) with p-value 0.00. The p-values for all coefficients were less than 0.05, thus the Chabahar station had a weak negative correlation with the atmospheric pressure. The weak correlation coefficients meant that the Oman Sea mean level at Chabahar station did not respond to atmospheric pressure as an inverse barometer effect, or strong deviation from isostatic response was observed. The non-barometric response to local atmospheric pressure partly represented an influence of sea level anomalies farther east due to the alongshore component of wind stress and it generally forced a large response than the onshore component. This was consistent with that expected from Ekman dynamics and upwelling (Figure 1). But, the ocean response to atmospheric pressure variations was close to the isostatic ones at Jask (r =-0.75), the response depended on the water flux dynamics at the Hormuz strait.

In the open ocean and for periods longer than a few days, the sea level response to atmospheric pressure forcing was close to an isostatic response (Fu and Pihos, 1994; Gaspar and Ponte, 1997) and is well known by an inverse barometer effect: a 1-mbar increased in atmospheric pressure induced a sea level decrease of 1.01 cm. Ducet et al. (1999) examined the validity of the inverse barometer approximation for the Black Sea mean level using 5 years of Topex/POSEIDEN data. They found very significant deviations from the inverse barometer response. They suggested that the deviation attributed to narrowness of the Bosphorus Strait and it had limiting role in water exchange. Also the Mediterranean mean sea level to atmospheric pressure departed from a standard inverse barometer effect due to the limiting role of the Strait of Gibraltar (Candela, 1991). Alothman et al. (2014) showed that at the Mina Sulman gauge there was no correlation between atmospheric pressure and sea level when the IB effect was subtracted from the data. Gomez-Enri et al. (2004) found that at mid and high latitudes in the Indian Ocean. They suggested that the relation between atmospheric pressure variations and sea level fluctuation (BF) values indicated a response near to the isostatic one; however, at low latitudes strong deviations from the isostatic response were observed. They observed some specific zones with values between 0.60 and 0.40 cm/mb, where the oceanic response was clearly far from isostatic (south of India, Thailand Gulf, south of Indonesia and the east region of Madagascar), contrary to that observed in the Atlantic Basin. Chabahr

located in low latitude in the north of the Indian Ocean, therefore the deviation from the isostatic response was expected.

Coherence Analysis between Atmospheric Pressure and Sea Level

In order to study the response of mean sea level at the Northern Coast of the Oman Sea to atmospheric pressure more fully, coherence between two parameters was observed. Coherence between atmospheric pressure and sea level is shown in Figure. 7. If the coherence value was unity, then the response of the sea level to the atmospheric pressure should be inverse barometer. It can be seen from Figure 7 that the coherence was unity. This means that in the northern coast the Oman Sea, mean sea level responded to atmospheric pressure as an inverse barometer at low frequencies. It can be noticed that the low correlation (-0.35) between atmospheric pressure and mean sea level found in the previous section was due to the combination of other interrelated physical parameters, such as air temperature, steric effect, evaporation, wind and Ekman transport, and this played an important role in mean sea level changes, interfering with the atmospheric pressure response. The behavior of the response of the Oman Sea mean level to atmospheric forcing at least in the northern coast was different from the one in the Persian Gulf because of the Hormuz strait, which was pure inverse barometer (Hassanzadeh et al., 2007).

Atmospheric Temperature and Wind

The correlation coefficients (r) between monthly sea-level and air temperature and wind data for Chabahar were 0.35 and 0.16, respectively. For Jask the correlation coefficient (r) between monthly sea-level and air temperature and wind data were 0.70 and 0.39, respectively. Hereafter, we present the same coherence analysis as before, but between the mean level of the Oman Sea and air temperature and wind at Chabahar station.

Results of the coherence analysis are shown on Figure 8 for mean sea level and air temperature. The most striking point to notice was the strong coherence, around 0.6, 0.8 and 1.0, for different periods with an almost steady gain at about 2.0., which meant that temperature had significant effect on mean sea level variations. The correlation between air temperature and atmospheric pressure showed that these parameters were highly inter-correlated. The same coherence analysis with the wind data was also performed, and this is shown in Figure 9. Interestingly, it lead to a much lower value at lower frequencies and noisier coherence at high frequencies, which meant that wind had no direct significant effect on mean sea level variations. The wind effect would yield water level proportional to wind stress, because of the associated Ekman transport and Ekman upwelling along the Iranian coast around the Chabahar Gulf as it can be seen from Figure 1.

The coherence analysis of the corresponding time series revealed an oscillatory behavior between mean sea level and other variables. The annual peak was dominant and contained the major energy in the time series and it can be seen for coherency of mean sea level and atmospheric pressure. The coherency between mean sea level and air temperature and wind indicated an annual and a semiannual signal. There were some coherency peaks at high and low frequencies which were not significant. The atmospheric pressure was minimum in summer while the temperature was maximum, and vice versa. It was obvious that the annual cycle was dominant in the atmospheric pressure and air temperature. There was also a weak semiannual cycle in the coherency of wind. This can be due to the variability associated with the strong monsoonal forcing over the northern Indian Ocean. The annual cycle was prominent in the wind speed.

Other Forces

In this section, we consider the Ekman dynamic in order to examine the wind forcing and also, the external factors, NAO and Monsoon that may affect the sea level in this area need be investigated. Sea level anomalies were affected by the global climate change as well as by abnormal local climate changes (Church et al., 2006). For example, Barzandeh et al. (2018) showed that the sea level anomaly responds to wind-driven coastal upwelling, as a regional phenomenon. The Ekman transport can be calculated in terms of wind stress, τ, sea water density, ρ_w=1025 $kg\ m^{-3}$, a dimensionless drag coefficient, C_d=1.4×10^{-3}, and air density, ρ_a=1.22 $kg\ m^{-3}$, with the following formula:

$$Q_x = \frac{\tau_y}{\rho_w f} \qquad \text{Eq.(7)}$$

$$Q_y = -\frac{\tau_x}{\rho_w f} \qquad \text{Eq.(8)}$$

where, wind stress components are:

$$\tau_x = \rho_a C_d \left(\sqrt{w_x^2 + w_y^2}\right) w_x \qquad \text{Eq.(9)}$$

and

$$\tau_y = \rho_a C_d \left(\sqrt{w_x^2 + w_y^2}\right) w_y \qquad \text{Eq.(9)}$$

f is the Coriolis parameter defined as twice the vertical component of the Earth's angular velocity, Ω, about the local vertical given by f=2Ωsin(θ) at latitude θ. Finally, the x subscript co rresponds to the zonal component and the y subscript to the meridional one. EOF analysis was used to study for spatial and temporal linked variability by analyzing mean sea level and Ekman transport. This method partitioned the temporal variance of the

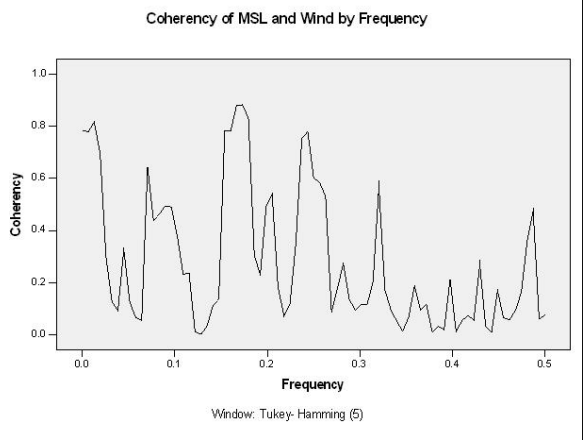

Figure 9. Coherence between mean sea level and wind of the Oman Sea for Chabahar station (Frequency, cycles/month)

highly correlated data into a small number of orthogonal spatial patterns called eigenvectors and corresponding orthogonal time coefficients. These Eigen functions have a series of coefficients in time that modulate them are ranked in decreasing order according to the percent of the variance. In general, each mode has an associated variance, non-dimensional spatial pattern, and dimensional time series. The set of orthogonal functions are derived from the data itself. The first eigenvector is virtually the same as an overall average pattern of Ekman transport in this case. The Ekman transport input data steps on n grid points.

The initial EOF analysis was performed on the Ekman transport. The results of the analysis demonstrated that over 48.90% of the mean square of the data was contained in the first function and that 87.16% of the mean square was captured by the first four modes of east-west component. Also, it demonstrated that over 48.20% of the mean square of the data was contained in the first mode and that 94.70% of the mean square the data was captured by the first fourth of the north-south component of the Ekman transport.

The correlation coefficients (r) of sea level with Ekman transport were found for both stations. Significant correlation coefficients, r=-0.70 (p-value=0.00) for Chabahar, and r=-0.40 (p-value =0.00) for Jask. The North Atlantic Oscillation (NAO) was recognized as the foremost mode of variability in the North Atlantic region with major impacts in Europe and further afield (Hurrell, 1995; Cullen and deMenocal, 2000) especially in the winter. Sea level in Black Sea was significantly correlated with winter NAO only in spring (Tsimplis et al., 2004), but sea level in the Persian Gulf was not correlated with the winter NAO index (Hassanzadeh et al., 1995). The

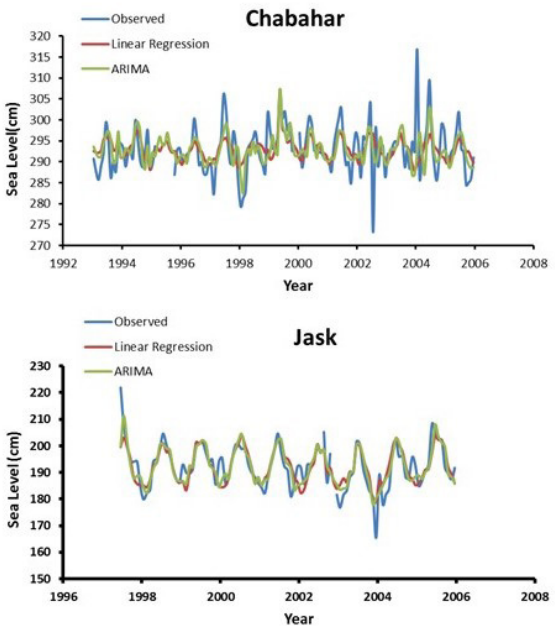

Figure 10. Comparison of fitted linear regression and ARIMA models with the observation

contributions of linear change and the NAO to sea-level variability in the northern coast of the Oman Sea were investigated in this study.

The monthly NAO indices of each year was used, which are represented by the sea-level difference between Azores atmospheric pressure High and Icelandic Low. The correlation coefficients (r) between monthly NAO and monthly sea-level data for Chabahar was r =-0.05 and for Jask it was r =-0.07. The p-values for all coefficients were less than 0.05, thus both stations had a weak negative correlation with the NAO.

Correlation coefficients between time series of Indian summer monsoon index and sea-level was calculated. The correlations coefficients, r =0.26 p = 0.12, for Chabahar and r =-0.07 p = 0.73, for Jask were obtained. Thus the sea-level at these tide gauges was little affected by Indian Ocean Monsoon. The sea level change appears to response to the Ekman transport which would be expected from the wind stress regimes. Sea level response to NAO and Monsoon was negligible compared with the response to regional forcings. EOF analyses was performed to find relations between the sea level and the Ekman transport. In the following, the Ekman transport variability is discussed in terms of the four time series of the leading PC mode.

Conclusion

The correlation analysis showed that the response of the Oman Sea mean level was deviated from inverse barometer. The coherence analysis revealed a significant coherence value between sea level and atmospheric pressure and did not validate the non-inverse barometer effect. Other causes of sea level variation in this region, such as steric effects associated with non-propagating seasonal variations or the existence of baroclinic Rossby and Kelvin waves in the Indian Ocean. It seemed that importance can be explained by the inverse barometer deviation. The departure from inverse barometer was due to the combination of other interrelated physical processes, such as air temperature, steric effect, evaporation, wind and Ekman transport, which played an important role in mean sea level changes and interfering with the atmospheric pressure response. Sea level response to NAO and Monsoon was negligible compared with the response to regional forcings.

The linear regression model was fitted to the mean sea level and forcing functions and ARIMA (2,0,2) models used various lagged values to forecast mean sea level. The accuracy of the forecasted using ARIMA is better than linear regression models.

Acknowledgement

The authors gratefully acknowledge the support of the Department of Research and Technology of University of Isfahan for this work. Moreover, we thank the Department of Oceanography and Prof. G. Weatherly, for hosting visits to Florida State University, Tallahassee, FL, when this work was carried out.

References

Alothman GO, Bos, MS, Fernandes, RMS, M.E. Ayhan, ME. (2015). Sea level rise in the north-western part of the Arabian Gulf. Journal of Geodynamics 81: 105–110.

Barzandeh A, Eshghi N, Hosseinibalam F, and Hassanzadeh S. (2018). Wind-driven coastal upwelling along the northern shoreline of the Persian Gulf. Bollettino di Geofisica Teorica e Applicata 59: 301-312.

Box GEP, Jenkins GM. (1976). Time series analysis: forecasting and control. Holden-Day, San Francisco, USA.

Candela J. (1991). The Gibraltar Strait and its role in the dynamics of the Mediterranean Sea. Dynamics of Atmospheres and Oceans 15(3-5): 267-299.

Church JA, White NJ, Hunter JR. (2006). Sea-level rise at tropical Pacific and Indian Ocean Islands. Global Planetary Change 5: 155-168.

Cullen HM, deMenocal PB. (2000). North Atlantic influence on Tigris-Euphrates stream flow. International Journal of Climatology 20: 853–863.

Ding X, Zheng D, Chen Y, Chao J, Li Z. (2001). Sea level change in Hong King from tide gauge measurements of 1954-1999. Journal of Geodesy 74: 683-689.

Eshghi N, Barzandeh A, Hosseinibalam F, Hassanzadeh, S. (2020). Investigating dynamic and static aspects of regional sea level changes in the north-western Indian Ocean, Bollettino di Geofisica Teorica e Applicata 61(2): 249-270.

Fu LL, Pihos G. (1994). Determining the response of sea level to atmospheric pressure forcing using TOPEX-rPOSEIDONdata. Journal of Geophysical Research 99: 24633–24642.

Gaspar P, Ponte R. (1997). Relation between sea level and barometric pressure determined from altimeter data and model simulations. Journal of Geophysical Research 102: 961–971.

Gomez-Enri J, Villares P, Brouno M, Catalan M. (2004). Evidence of different ocean responses to atmospheric pressure variations in the Atlantic, Indian and Pacific Basin as deduced from ERS-2 altimeter data. Annales Geophysicae 22: 331-345.

Gomis D, Ruiz S, Sotillo GM, Alvarez-Fanjul E, Terradas J. (2008). Low frequency Mediterranean sea level variability: The contribution of atmospheric pressure and wind. Global and Planetary Change 83: 215-229.

Hassanzadeh S, Kiasatpour A, Hosseinibalam F. (2007). Sea-level response to atmospheric forcing along the north coast of Persian Gulf. Meteorology and Atmospheric Physics 95: 223-237.

Haredide D. (2004). Iranian Tide Gauge Network IOC/GLOSS, Technical Report (http://www.pol.ac.uk/psmsl/reports.gloss/general/).

Hosseinibalam F, Hassanzadeh S, Kiasatpour A. (2007). Interannual variability and seasonal contribution of thermal expansion to sea level in the Persian Gulf. Deep-Sea Research I 54: 1474–1485.

Hurrell JW. (1995). Decadal trends in the North Atlantic Oscillation: Regional temperatures and precipitation. Science 269: 676–679.

Johns EW, Jacobs AG, Kindle CJ, Murray PS, Carron M. (1999). Arabian Marginal seas and Gulf. Report of a Workshop held at Stennis Space Center, Mississippi, USA.

Juncheng Z, Jianli Z, Ling D, Peiliang L, Lei L. (2009). Global sea level and thermal contribution. Journal of Ocean University of China 8(1): 1-8.

Preisendorfer RW. (1988). Principal component analysis in meteorology and oceanography. Developments in Atmospheric Science, Elsevier, Netherlands, 425 pp.

Sawa T. (1978). Information criteria for discriminating among alternative regression models. Econometrica 46:1273–1291.

Siddig NA, Al-Subhi, A. M., Alsaafani, M. A. (2019). Tide and mean sea level trend in the west coast of the Arabian Gulf from tide gauges and multi-missions satellite altimeter. Oeanologia 218: 1-11.

Stammer D, Cazenave A, Ponte RM, Tamisiea, ME. (2013). Causes for contemporary regional sea level changes. Annual Review of Marine Science 5: 21-46.

Somot S, Sevault F, Deque M. (2006). Transient climate change scenario simulation of the Mediterranean Sea for the 21st century using a high-resolution ocean. Climate Dynamics 27: 851–879.

Tsimplis MN, Josey SA, Rixen M, Stanev EV. (2004). On the forcing of sea-level in the Black sea. Geophysical Research Letters 109: C08015.

Wunsch C. (1972). Bermuda sea level in relation to tides, weather, and baroclinic fluctuations. Reviews of Geophysics 10: 1–49.